Optimal Control of a Tumor-Immune System with a Modified Stepanova Cancer Model

Maria Dassow, Seddik Djouadi, Kaouther Moussa

Optimal Control of a Tumor-Immune System with a Modified Stepanova Cancer Model

Maria Dassow* Seddik Djouadi Kaouther Moussa*****

*Univ. of Tennessee, Knoxville, TN. {email: mdassow@vols.utk.edu}
**Univ. Of Tennessee, Knoxville, TN {email: mdjouadi@utk.edu}
***Univ. Grenoble Alpes, CNRS, Grenoble INP, GIPSA-lab, 38000 Grenoble, France {email: kaouther.moussa@gipsa-lab.fr}

Abstract: In this paper, we investigate strategies for administering chemo- and immunotherapy to force a tumor-immune system to its healthy equilibrium. To solve this problem, we use Pontryagin's Maximum Principle applied to a modified Stepanova model. This model directly accounts for the detrimental effects of chemotherapy on immune cell density. Because the parameter for this interaction is unknown, we run simulations while varying the parameter to observe the effect on the system. Our results show that combined dosages of chemo- and immunotherapy over the first days of the treatment period are sufficient to force the system to its healthy equilibrium.

Keywords: cancer, chemotherapy, immunotherapy, drug delivery, biological systems, optimization, Pontryagin's Maximum Principle

1. INTRODUCTION

Since their creation, the tools of mathematical optimization have been indispensable in predicting and controlling the behavior of systems. Optimal control techniques can be applied to a range of systems and are useful in a variety of fields including economics, engineering, and physics. As control methods have evolved, they have been used to describe biological models, which are often highly complex and nonlinear. In this paper, we focus on a biological model that describes the interactions between cancer and immune cells as they undergo various types of therapy. Our aim is to find the optimal doses of each therapy to drive the tumor-immune system to a benign state.

The two therapies considered in this paper are chemotherapy and immunotherapy. Chemotherapy attacks the different types of cells (tumor and immune cells) while immunotherapy increases the density of immune cells. The purpose of immunotherapy is to boost the immune system so that it can better fight the growth of tumor cells. Although immunotherapy has been used as a supplement to chemotherapy, Koebel et al. (2007) proposed that immunotherapy alone can drive the tumor to a healthy state for some given initial health conditions.

Because both therapies have negative side effects, it is necessary to limit their administration. Thus, most classic optimal control methods for tumor-immune system dynamics design the cost function to minimize the tumor density as well as the amount of drugs administered (Ledzewicz et al., 2020). This technique operates off an *implicit* understanding that excessive immunotherapy and chemotherapy are harmful to the body. In this paper, however, we consider a model of tumor-immune dynamics that *explicitly* accounts for the damage chemotherapy inflicts on the immune system (de Pillis et al, 2007). By incorporating the side effects of chemotherapy directly, we are ensuring that the negative side effects are accounted for so that our model more accurately represents the tumor-immune system dynamics. Furthermore, this model has been used to design model predictive control strategies, see for example Sharifi (2017, 2020).

In this paper, we use the model presented by Moussa et al. (2020) to solve the optimal control problem using Pontryagin's Maximum Principle with both L_1 and L_2 type objective functions. Each type of function has its benefits and its disadvantages. Quadratic cost functions ensure that the Hamiltonian will be convex with a global minimum. It is often easy to manipulate such cost functions and to derive information from them. However, using quadratic terms may have the effect of warping the data (Ledzewicz & Schättler, 2007). Whereas quadratic cost functions result in smooth functions, linear cost functions give *bang-bang* controls. In this type of function, the control is either at full strength or zero strength with possible singular arcs in between. This dosing schedule mimics real life administration of drugs but is much more difficult to derive (Swierniak et al., 2003). Here, we compare the optimal control of both cost functions to identify the best dosing schedule.

The rest of this paper is organized as follows; in section 2 the tumor-immune system model is presented. In section 3, the nonlinear controllability of the system is determined. In section 4, the L_2 optimal control problem is solved, and the

corresponding system response presented with Monte-Carlo simulations. In section 5, the L_1 optimal control problem is solved, and numerical response presented. Section 6 contains concluding remarks and future work.

2. THE TUMOR-IMMUNE SYSTEM

The model we investigate here is a modified version of the Stepanova model that has been extensively used in literature where optimal control approaches were proposed to schedule chemo- and immunotherapy injection profiles (Stepanova, 1980; d'Onofrio, 2012; Ledzewicz et al., 2012; Ledzewicz et al., 2020). Sharifi et al. (2017) proposed a multiple model predictive control scheme to design chemo- and immunotherapy injection schedules. Furthermore, Sharifi et al. (2020) proposed a robust multiple model predictive control scheme for this model, in order to consider direct drug targeting pharmacokinetic uncertainties as well as system model mismatches. Because biological systems are intricate, models of these systems can become too complex to analyze and manipulate. The model we use is minimally parameterized; however, it still describes the main aspects of tumor-immune interactions (Moussa et al. 2020). Included in the Stepanova model is a growth rate of the tumor cells. While both Gompertzian and exponential growth rates have been used in various Stepanova models, we use a logistic growth model. This growth rate accounts for limited carrying capacity, reflecting the physical limits of tumor cell density.

The system used in this paper, introduced by Moussa et al. (2020), is a modified form of the classic Stepanova model:

$$\begin{aligned} \dot{x_1} &= \mu_C x_1 - \frac{\mu_C}{x_\infty} x_1^2 - \gamma x_1 x_2 - \kappa_x x_1 u_1 \\ \dot{x_2} &= \mu_I (x_1 - \beta x_1^2) x_2 - \delta x_2 + \alpha + \kappa_y x_2 u_2 - \eta u_1 x_2 \end{aligned} \tag{1}$$

Here x_1 represents the number of tumor cells and x_2 the immune cell density. The controls, u_1 and u_2, represent the administration of chemo- and immunotherapy, respectively. We extend the Stepanova model with the term $\eta u_1 x_2$, which represents the interaction between chemotherapy and immune cells and directly accounts for the detrimental effect of chemotherapy on the immune system (Moussa et al., 2020). In this paper, we will set $\eta = 1$, unless otherwise stated. Later we will consider the control problem while varying η. We assess a method for random sampling that remains applicable for other uncertain parameters. Table 1 provides the numerical values for the parameters used in the model with the state variables having been normalized (d'Onofrio et al., 2012).

Table 1: Numerical values for the system variables

Parameter	Definition	Numerical value
μ_C	tumor growth rate	$0.5599 \cdot 10^7$ cells/day
μ_I	tumor stimulated proliferation rate	0.00484 day^{-1}
α	rate of immune cells influx	0.1181 day^{-1}
β	inverse threshold	0.00264
γ	interaction rate	$1 \cdot 10^7$ cells/day
δ	death rate	0.37451 day^{-1}
κ_X	chemotherapeutic killing parameter	$1 \cdot 10^7$ cells/day
κ_Y	immunotherapy injection parameter	$1 \cdot 10^7$ cells/day
x_∞	fixed carrying capacity	$780 \cdot 10^6$ cells

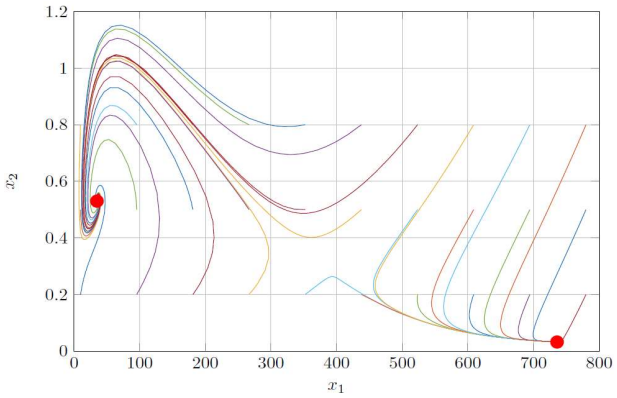

Figure 1: Phase portrait of the uncontrolled system showing the two locally asymptotically stable equilibrium points (Moussa, 2020).

2.1 Dynamics of the Uncontrolled System

As predicted by Koebel (2007), the uncontrolled system $(u_1, u_2 = 0)$ has a benign equilibrium in which the tumor subsists in a microscopic state. The healthy equilibrium is at $(x_1, x_2) = (34.98, 0.53)$, while an unhealthy equilibrium exists at $(x_1, x_2) = (735.9, 0.032)$, see Figure 1. We will consider the control problem starting from the initial condition $(x_1, x_2) = (500, 0.5)$, which would tend to the unhealthy equilibrium in the absence of therapy. The amount of chemo- and immunotherapy needed to drive the system to the healthy equilibrium heavily depends on the initial condition.

3. CONTROLLABILITY OF THE SYSTEM

Before attempting to control a system, it is necessary to determine whether the system is in fact controllable. Our system can be represented as

$$\begin{cases} \dot{x} = f\big(x(t), u(t)\big) = f(x) + g_1(x)u_1(t) + g_2(x)u_2(t) \\ y = h\big(x(t)\big), \; x(0) = x^0 \end{cases} \tag{2}$$

where

$$g_1 = \begin{bmatrix} \kappa_x x_1 \\ -\eta x_2 \end{bmatrix}, \; g_2 = \begin{bmatrix} 0 \\ \kappa_y x_2 \end{bmatrix}$$

For nonlinear systems, controllability is defined in terms of accessibility. We say that, given a system and an initial state x^0, if it is possible to choose a control $u(t)$ to drive the system to another state x^1, then x^1 is accessible from x^0. If all states are accessible from every other state, then the system is controllable (James, 1987).

One criterion for determining controllability is the controllability rank condition. In a neighborhood M of x^0, if $dim < ad_f \mid R(f) >= n$, where n is the dimension of x, then the system satisfies the controllability rank condition (Bara, 2017). Here $< ad_f \mid R(f) >$ is the controllability distribution where ad_f represents the adjoint, and $R(f)$ is the distribution spanned by $f(\cdot, u)$ (Isidori, 1995). This condition can be verified using the controllability matrix defined as

$$C = (g_1, g_2, [g_1, g_2], \dots) \tag{3}$$

where $[g_1, g_2]$ is the Lie bracket (Hermann & Krener, 1977). The Lie bracket is closely connected to controllability and defines a new vector field. A Lie bracket is calculated and defined as (Hedrick & Girard, 2005):

$$[g_1, g_2] \equiv \frac{\partial g_2}{\partial x} f - \frac{\partial g_1}{\partial x} g \tag{4}$$

If the controllability matrix C has rank n at x_0, then the system is locally controllable around x_0. Since our model has rank 2, we only need to check if this matrix has rank 2 around the equilibrium points. Thus, if we take only the first two columns in the controllability matrix, and it has rank 2, then the condition is verified.

$$C = (g_1, g_2) = \begin{bmatrix} \kappa_x x_1 & 0 \\ -\eta x_2 & \kappa_y x_2 \end{bmatrix} \tag{5}$$

These vectors are already linearly independent and will therefore be trivially full rank. By plugging in the equilibrium points, we obtain the following full rank matrices, C_1 and C_2, corresponding to the healthy and unhealthy equilibrium, respectively.

$$C_1 = \begin{bmatrix} 349800000 & 0 \\ -53/100 & 5300000 \end{bmatrix}$$

$$C_2 = \begin{bmatrix} 7359000000 & 0 \\ -4/125 & 320000 \end{bmatrix}$$

Because these controllability matrices have rank 2, our system is locally controllable around both equilibrium points. With this information, we can proceed to derive controls to force the system to the healthy equilibrium.

4. L_2 OPTIMIZATION

The optimal control problem for this system was solved by Moussa et al. (2012) using the generalized moment approach developed by Lasserre. In this paper, however, we use Pontryagin's Maximum Principle to solve the optimal control problem with both L_1 and L_2 type objective functions. For both solutions, it is necessary that $x_1, x_2 \geq 0$ to reflect physical realities. In addition, the immune cell density must remain relatively high to ensure the health of the entire body. We will consider here that $x_1 > 0.1$ at all times.

4.1 Methods for L2 Optimal Control

In this section, we explore the optimal controls for a quadratic cost function (Lenhart & Workman, 2007):

$$J(u, v) = \int_0^T (x^T Q x + u^T R u) dt = \int_0^T (q_1 {x_1}^2 + q_2 {x_2}^2 + r_1 {u_1}^2 + r_2 {u_2}^2) dt \tag{6}$$

$$Q = \begin{bmatrix} q_1 & 0 \\ 0 & q_2 \end{bmatrix} = \begin{bmatrix} 1 & 0 \\ 0 & 0 \end{bmatrix}, \; R = \begin{bmatrix} r_1 & 0 \\ 0 & r_2 \end{bmatrix} = \begin{bmatrix} 10^6 & 0 \\ 0 & 10^6 \end{bmatrix}$$

The weights represented in matrices Q and R can be chosen to penalize certain parameters more or less as desired. The weights for r_1 and r_2 penalize the use of drugs to minimize the injected doses. We do not put a weight on the immune cells ($q_2 = 0$), as we do not want them to be minimized. The Hamiltonian for this cost function is as follows:

$$H = q_1 {x_1}^2 + q_2 {x_2}^2 + r_1 {u_1}^2 + r_2 {u_2}^2 + \lambda_1 \left(\mu_C x_1 - \frac{\mu_C}{x_\infty} x_1^2 - \gamma x_1 x_2 - \kappa_x x_1 u_1\right) + \lambda_2 \left(\mu_I x_1 x_2 - \mu_I \beta x_1^2 x_2 - \delta x_2 + \alpha + \kappa_y x_2 u_2 - \eta u_1 x_2\right) \tag{7}$$

The corresponding adjoint equations:

$$\dot{\lambda_1} = -\frac{\partial H}{\partial x_1} = -2q_1 x_1 + \lambda_1 \left(-\mu_C + 2\frac{\mu_C}{x_\infty} x_1 + \gamma x_2 + \kappa_x u_1\right) + \lambda_2 (-\mu_I x_2 + 2\mu_I \beta x_1 x_2) \tag{8}$$

$$\dot{\lambda_2} = -\frac{\partial H}{\partial x_2} = -2q_2 x_2 + \lambda_1 \gamma x_1 + \lambda_2 \left(-\mu_I x_1 + \mu_I \beta x_1^2 + \delta - \kappa_y u_2 + \eta u_1\right) \tag{9}$$

The optimality conditions can be found as follows:

$$\frac{\partial H}{\partial u_1} = 2r_1 u_1 - \lambda_1 \kappa_x x_1 - \lambda_2 \eta x_2 = 0$$

$$u_1 = \frac{\lambda_1 \kappa_x x_1 + \lambda_2 \eta x_2}{2r_1} \tag{10}$$

$$\frac{\partial H}{\partial u_2} = 2r_2 u_2 + \lambda_2 \kappa_y x_2 = 0$$

$$u_2 = \frac{-\lambda_2 \kappa_y x_2}{2r_2} \tag{11}$$

To solve these equations numerically, we discretized the system and used the Forward-Backward Sweep method (Lenhart & Workman, 2007). This algorithm works as follows:

1. Make an initial guess for the controls u over the interval (u = 0 typically works well).
2. Solve the state equations numerically forward in time using the initial condition $x_1 = x(t_0)$ and the initial guess for u.
3. Solve the adjoint equations numerically backward in time.

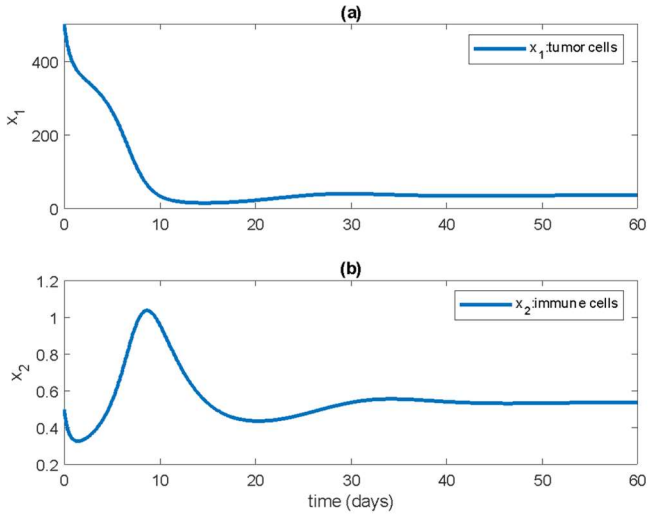

Figure 2: The trajectory of the tumor (a) and immune cell (b) density under the influence of the controls.

using the transversality condition, $\lambda(N+1) = \lambda(T) = 0$, and the values for u and x.

4. Update the value of the controls using the new values for x and λ.

5. Check for convergence of each of these parameters. Repeat steps 1-4 until the state, adjoint, and control functions are negligibly close.

For steps 2 and 3, we used the 4th order Runge-Kutta method to solve for the state and adjoint equations numerically.

4.2 Numerical Results with L_2 Objective

Figures 2 and 3 display the results of our Forward-Backward Sweep, giving the optimal controls to drive the system to its healthy equilibrium for the initial condition $(x_1, x_2) = (500, 0.5)$. Figure 2 shows the trajectories of the tumor and immune cell densities under the influence of the controls. Both states are driven to the healthy equilibrium, and x_2 naturally remains above the healthy threshold $(x_2 > 0.1)$. Figure 3

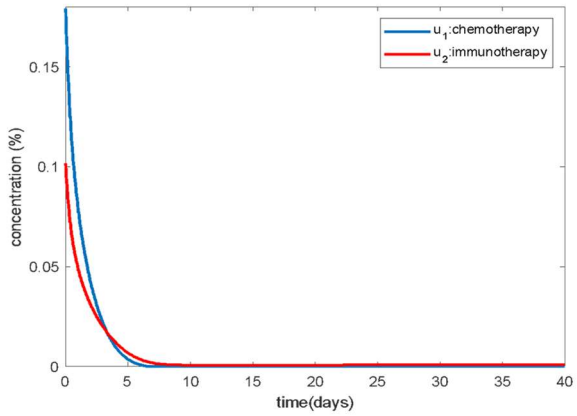

Figure 3: Control profiles for L_2 objective, where u_1 represents chemotherapy, and u_2 represents immunotherapy.

shows the scheduling and dosage of the chemo- and immunotherapy that forces the system to its healthy state.

For approximately the first 5 days, chemotherapy is administered at a higher concentration than immunotherapy. Then, once the immune cell density has decreased below its equilibrium amount, immunotherapy dosage increases to higher levels than chemotherapy, allowing the immune system to rebuild itself and recover from chemotherapy. The immune cell density never drops to dangerously low levels, and both states remain nonnegative.

4.3 Monte-Carlo Simulations

Because the parameter η is unknown, we now explore the effect different values of η have on the control problem. To analyze this effect, we perform Monte-Carlo simulations. We run the same numerical method to solve the optimal control problem, but we vary η, taking 20 random values between 0 and 2, assuming $\eta \sim U([0,2])$.

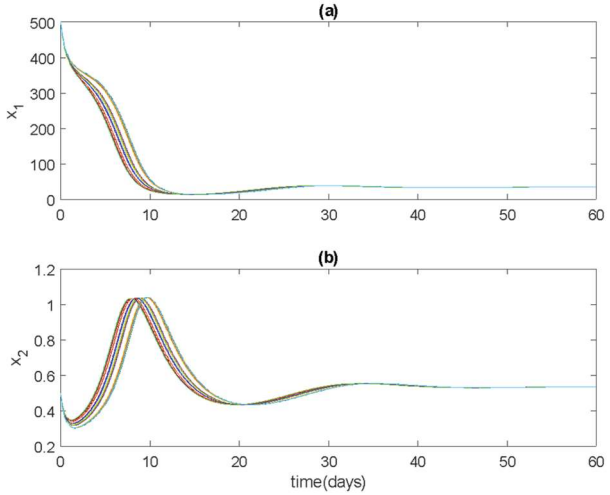

Figure 4: Results of the Monte-Carlo simulations showing the profiles of the tumor cell number (a), the immune cell density (b)

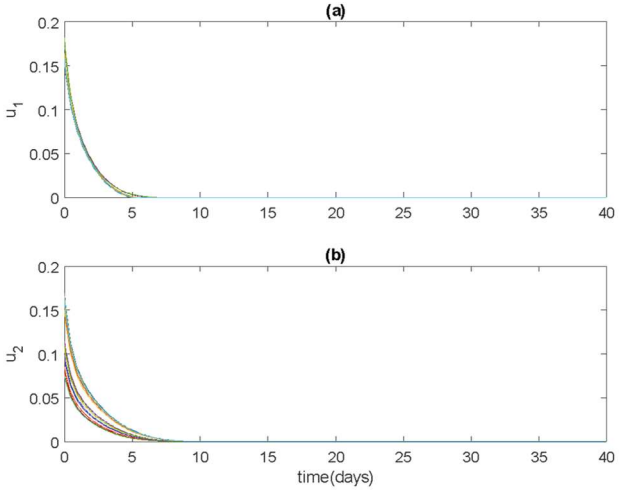

Figure 5: Results of the Monte-Carlo simulations showing the administration of chemotherapy (a) and immunotherapy (b)

Figures 4 and 5 show the results of the Monte-Carlo simulations. Overall, the system behaves similarly over all values of η. The states remain nonnegative, and the immune cell density remains within a healthy range. In each trial, the tumor and immune cells reached their healthy equilibrium, and the trajectories only had slight deviations. The immunotherapy profiles show more dispersion across the simulation than the chemotherapy profiles. Looking at the system dynamics in (1), it is probable that the immunotherapy doses increase as η increases.

5. L_1 OPTIMIZATION

In this section, we will solve the optimal control problem with an L_1, or linear, objective function. Using a linear objective function more closely reflects real-world systems. However, it is more difficult to derive the controls with a linear function.

5.1 Methods for L_1 Optimal Control

For an L_1 objective, the cost function is as follows [11]:

$$J(u,v) = \int_0^T |Qx + Ru|dt = \int_0^T |q_1x_1 + q_2x_2 + r_1u_1 + r_2u_2|\, dt \tag{12}$$

Using Pontryagin's Maximum Principle, we derive the following Hamiltonian function with its corresponding adjoint functions:

$$H = q_1x_1 + q_2x_2 + r_1u_1 + r_2u_2 + \lambda_1\left(\mu_C x_1 - \frac{\mu_C}{x_\infty}x_1^2 - \gamma x_1x_2 - \kappa_x x_1u_1\right) + \lambda_2\left(\mu_I x_1x_2 - \mu_I\beta x_1^2x_2 - \delta x_2 + \alpha + \kappa_y x_2u_2 - \eta u_1x_2\right) \tag{13}$$

$$\dot{\lambda_1} = -\frac{\partial H}{\partial x_1} = -q_1 + \lambda_1\left(-\mu_C + 2\frac{\mu_C}{x_\infty}x_1 + \gamma x_2 + \kappa_x u_1\right) + \lambda_2(-\mu_I x_2 + 2\mu_I\beta x_1x_2) \tag{14}$$

$$\dot{\lambda_2} = -\frac{\partial H}{\partial x_2} = -q_2 + \lambda_1\gamma x_1 + \lambda_2\left(-\mu_I x_1 + \mu_I\beta x_1^2 + \delta - \kappa_y u_2 + \eta u_1\right) \tag{15}$$

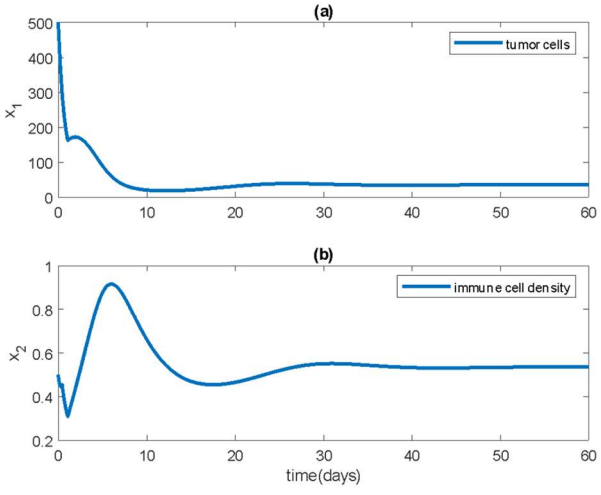

Figure 6: The trajectories of the tumor cells (a) and the immune cell density (b) using an L_1 objective.

Here, unlike with the L_2 objective, the controls do not appear in the optimality condition since they are linear in the Hamiltonian. Thus, it is impossible to explicitly solve for them. Instead of solving for u_1 and u_2, we must use switching functions (d'Onofrio et al., 2012). The switching function for u_1 is defined as

$$\psi_1 = \frac{\partial H}{\partial u_1} = r_1 - \lambda_1\kappa_x x_1 - \lambda_2\eta x_2 \tag{16}$$

where

$$u_1 = \begin{cases} 0 & if\ \psi_1(t) > 0 \\ 1 & if\ \psi_1(t) < 0 \end{cases} \tag{17}$$

The switching function for u_2 is defined as

$$\psi_2 = \frac{\partial H}{\partial u_2} = r_2 + \lambda_2\kappa_y x_2 \tag{18}$$

where

$$u_2 = \begin{cases} 0 & if\ \psi_2(t) > 0 \\ 1 & if\ \psi_2(t) < 0 \end{cases} \tag{19}$$

These controls have the extreme values of 0 and 1, jumping between full and zero doses depending on the sign of the switching functions. Such controls are called *bang* controls (d'Onofrio et al., 2012). If the controls switch more than once, they are called a *bang-bang* controls. When $\psi = 0$, the control is called singular and must be found using other methods. The theory for finding singular arcs can be quite complex and is explored by Bonnard and Chyba (2003). Our system was checked for singular controls while being numerically solved, and no singular arcs existed. As with the L_2 objective, we used the Forward-Backward Sweep method; however, we used gradient descent to solve for the state and adjoint equations.

5.2 Numerical Results with L_1 Objective

Figures 6 and 7 show the results of optimization using a linear objective function starting from the initial condition $(x_1, x_2) = (500, 0.5)$. In these graphs, the system is driven to its healthy equilibrium by the bang controls. Here, chemotherapy is administered for a day at full strength, and immunotherapy is

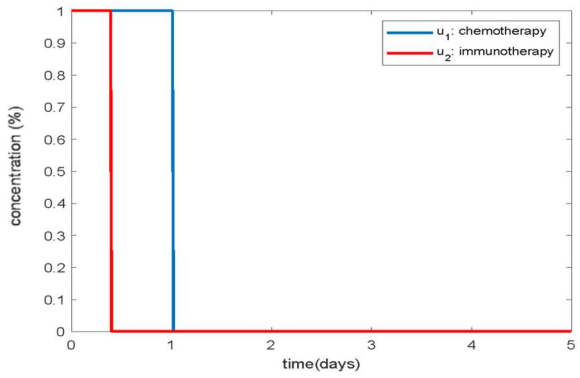

Figure 7: The scheduling for chemotherapy in blue and immunotherapy in red using the L_1 objective. Only the first 5 days are shown as there is no therapy for the remainder of the treatment period.

administered for around half a day at full strength to drive the system to its healthy state.

As with the L_2 objective function, both therapies are administered in combination here for the optimal effect. Additionally, all parameters remain within their constraints. In Figure 7, the therapy profiles are only shown for the first five days as they remain at zero for the rest of the treatment period.

6. CONCLUSION

Our results suggest that a combination of chemo- and immunotherapy sustained for a short period of time at the beginning of the treatment period is optimal for driving the tumor-immune system to its healthy equilibrium. This pattern is consistent across L_1 and L_2 objectives. These results are ideal when considering real-life treatment plans and for minimizing the damaging side effects of the therapies. Our results also reflect the results of the control problem with the same system found by Moussa et al. (2020) and with a similar Stepanova model found by d'Onofrio et al. (2012). In both papers, as in this one, immunotherapy alone was not found to be the optimal treatment. Instead, a mixture of both therapies was best in moving the system from its malignant initial condition to its healthy equilibrium. These results are reasonable when considering the ultimate goal of attacking the tumor cells while also supporting the immune system.

With both objective functions, a relatively short administration period was enough to drive the system away from its malignant equilibrium. Further research would be necessary to determine how the controls would change based on different initial conditions and to investigate what initial conditions are viable for treatment.

Our results from the Monte-Carlo simulations show that varying the unknown parameter η changed the optimal doses of immunotherapy. Otherwise, varying this parameter had little effect on the outcome of the control problem, thus suggesting that the system will behave similarly if the parameter is within the distribution we tested. For further research, it would be necessary to run clinical tests to find the value of this parameter. Clinically finding a value for the parameter describing the chemo-immune system interaction would greatly increase the validity of this model. Additionally, further research could be done to verify these results across varying types of chemo- and immunotherapy.

REFERENCES

Bara, O. (2017) Nonlinear Control and Estimation of an Inflammatory Immune Response. PhD diss., University of Tennessee.

Bonnard, B., Chyba, M. (2003). Singular Trajectories and their Role in Control Theory. *Mathématiques & Applications*, 40, Springer, Paris.

d'Onofrio, A., Ledzewicz, U., and Schättler, H. (2012). On the Dynamics of Tumor-Immune System Interactions and Combined Chemo- and Immunotherapy. Springer Milan, pp. 249–266.

De Pillis, L.G., Gu, W., Fister, K.R., et al. (2007). Chemotherapy for tumors: an analysis of the dynamics and a study of quadratic and linear optimal controls. *Mathematical Biosciences*. 209(1), pp. 292-315.

Hedrick, J.K. & Girard, A. (2005). Control of nonlinear dynamic systems theory and applications. Class Notes. pp.62-83.

Hermann, R, and A Krener. (1977). Nonlinear Controllability and Observability. *IEEE transactions on automatic control,* 22, 5, pp. 728–740.

Isidori, A. (1995). *Nonlinear control systems*, 1, Springer Science & Business Media.

James, M.R. (1987). Controllability and Observability of Nonlinear Systems. Mathematics Department and Systems Research Center, University of Maryland.

Koebel, C.M., Vermi, W., Swann, J.B., Zerafa, N., Rodig, S.J., Old, L.J., Smyth, M.J., Schreiber, R.D. (2007). Adaptive immunity maintains occult cancer in an equilibrium state. *Nature,* 450, pp. 903–907.

Ledzewicz, U. and Schättler, H. (2007). Optimal controls for a model with pharmacokinetics maximizing bone marrow in cancer chemotherapy. *Mathematical Biosciences*, 206(2), pp. 320–342.

Ledzewicz, U., and Schättler, H. (2020). On the Role of the Objective in the Optimization of Compartmental Models for Biomedical Therapies. *Journal of Optimization Theory and Applications,* 187, pp. 305–335.

Ledzewicz, U., Faraji, M., and Schättler, H. (2007). On optimal protocols for combinations of chemo- and immunotherapy. In 2012 IEEE 51st IEEE Conference on Decision and Control, pp. 7492–7497.

Lenhart, S. and Workman, J. T. (2007). *Optimal control applied to biological models*. RC Press.

Moussa, K., Fiacchini, M., Alamir, M. (2020). Robust Optimal Scheduling of Combined Chemo- and Immunotherapy: Considerations on Chemotherapy Detrimental Effects. American Control Conference.

Sharifi, N., Ozgoli, S., and Ramezani, A. (2017). Multiple model predictive control for optimal drug administration of mixed immunotherapy and chemotherapy of tumors. *Computer Methods and Programs in Biomedicine,* 144, pp. 13–19.

Sharifi, N., Zhou, Y., Holmes, G., and Chen, Y. (2020). Overcoming channel uncertainties in touchable molecular communication for direct-drug-targeting-assisted immuno-chemotherapy. *IEEE Transactions on NanoBioscience,* 19(2), pp. 249–258.

Stepanova, N. (1980). Course of the immune reaction during the development of a malignant tumour. *Biophysics*.

Swierniak, A., Ledzewicz, U., and Schattler, H. (2003). Optimal control for a class of compartmental models in cancer chemotherapy. *International Journal of Applied Mathematics and Computer Science*, 13(3), pp. 357–368.